Plant Biotechnology Journal
Open Access

Plant Biotechnology Journal (2023) **21**, pp. 979–989 doi: 10.1111/pbi.14009

Identification of *TaGL1-B1* gene controlling grain length through regulation of jasmonic acid in common wheat

Mohsin Niaz, Lingran Zhang, Guoguo Lv, Huiting Hu, Xi Yang, Yongzhen Cheng, Yueting Zheng, Bingyang Zhang, Xiangning Yan, Aye Htun, Lei Zhao, Congwei Sun, Ning Zhang, Yan Ren and Feng Chen*

National Key Laboratory of Wheat and Maize Crop Science, CIMMYT-China Wheat and Maize Joint Research Center, Agronomy College, Henan Agricultural University, Zhengzhou, China

Received 30 July 2022;
revised 15 December 2022;
accepted 6 January 2023.
**Correspondence* (Tel +86-37156990337; fax +86-37156990188; email fengchen@henau.edu.cn)

Keywords: common wheat, grain length, TaGL1, TaPAP6, carotenoid content, jasmonic acid.

Summary

Grain length is one of the most important factors in determining wheat yield. Here, a stable QTL for grain length was mapped on chromosome 1B in a F_{10} recombinant inbred lines (RIL) population, and the gene *TaGL1-B1* encoding carotenoid isomerase was identified in a secondary large population through multiple strategies. The genome-wide association study (GWAS) in 243 wheat accessions revealed that the marker for *TaGL1-B1* was the most significant among all chromosomes. EMS mutants of *TaGL1* possessed significantly reduced grain length, whereas *TaGL1-B1*-overexpressed lines possessed significantly increased grain length. Moreover, TaGL1-B1 strongly interacted with TaPAP6. *TaPAP6*-overexpressed lines had significantly increased grain length. Transcriptome analysis suggested that *TaPAP6* was possibly involved in the accumulation of JA (jasmonic acid). Consistently, JA content was significantly increased in the *TaGL1-B1* and *TaPAP6* overexpression lines. Additionally, the role of *TaGL1-B1* in regulating carotenoids was verified through QTL mapping, GWAS, EMS mutants and overexpression lines. Notably, overexpression of *TaGL1-B1* significantly increased wheat yield in multiple locations. Taken together, overexpression of *TaGL1-B1* enhanced grain length, probably through interaction with TaPAP6 to cause the accumulation of JA that improved carotenoid content and photosynthesis, thereby resulted in increased wheat yield. This study provided valuable genes controlling grain length to improve yield and a potential insight into the molecular mechanism of modulating JA-mediated grain size in wheat.

Introduction

Common wheat (*Triticum aestivum* L.) is one of the major staple cereals that dominate global agricultural production. By the year 2050, wheat yield must be conservatively increased by 60% to meet the demand of the growing population in the world (Shiferaw *et al.*, 2013). The genetic improvement of yield is a fundamentally long-term breeding objective in common wheat. Wheat yield is significantly determined by grain size (Nadolska-Orczyk *et al.*, 2017). Significant efforts have been made to elucidate the genetic mechanism governing wheat grain size. As a result, many QTLs/genes controlling grain size have been identified in polyploidy wheat (Guan *et al.*, 2018; Zhai *et al.*, 2018). However, only a few QTLs have been cloned (Simmonds *et al.*, 2014). A robust QTL (*Qtgw-cb.5A*) was associated with an increase of 6.9% in grain weight, which was predominantly caused by an increase of 4% in grain length (Brinton *et al.*, 2017). Recently, several wheat genes related to grain size have been successfully cloned by homology-based cloning. A *Positive Regulator Of Grain Size 1* (*TaPGS1*) as a homologue of *OsRc* (*brown pericarp and seed coat*) was cloned, and its overexpression lines increased grain length by 18.84% and grain weight by 13.81% (Guo *et al.*, 2022) in common wheat. *TaDA1-A* and *TaGW2-B* were identified as dominant-negative regulators of grain size because silencing of both genes had an additive effect, resulting in the increase of 5.7%–7.8% in grain length and 16.1%–20.8% in weight. Moreover, the combined effect of their favourable haplotypes (*TaDA1-A-HapI* and *TaGW2-B-HapI/II*) was far greater than the single effect (Liu *et al.*, 2020). Additionally, a number of positive regulators for grain size (e.g., *TaGS5-3A* and *TaSus1*) were reported to be significantly associated with grain size (Hou *et al.*, 2014; Ma *et al.*, 2016).

Grain size-related genes are predicted to be involved in diverse signal pathways, including phytohormone accumulation and starch biosynthesis (Zuo and Li, 2014). Hormones affect grain development during grain filling. Auxin affects the endosperm and seed coat. Increasing the expression of *PLA1/CYP78A1* in maize, *CYP78A13* in rice and *CYP78A5* in wheat significantly increased seed weight and yield by affecting auxin content (Guo *et al.*, 2022; Sun *et al.*, 2017; Xu *et al.*, 2015). As a member of the serine carboxypeptidase-like (SCPL) family, *GS5* modulates grain size through mediating brassinosteroid (BR) signal (Li *et al.*, 2011). *GL3.1/qGL3* is also involved in the BR signalling pathway to control grain length (Zhang *et al.*, 2012). *GS2* encoding *OsGRF4* negatively regulates the BR signal pathway and interacts with *OsGSK2* to inhibit its transcriptional activity (Che *et al.*, 2016). GW5 inhibits the phosphorylation and activity of GSK2 and participates in the BR signal pathway (Liu *et al.*, 2017). Jasmonic Acid (JA) is an essential plant hormone that fulfils critical roles in plant defence and development (Browse, 2009; Lyons *et al.*, 2013). A JA synthetic gene *KAT-2B* overexpression lines increase grain weight, thereby enhance yield (Chen *et al.*, 2020).

Overexpression of *TaSTT3b-2B* reveals a considerable increase in grain weight and innate immunity, indicating that JA biosynthesis is most likely responsible for the increased wheat grain size (Zhu *et al*., 2021).

Carotenoid isomerase (CRTISO) is a key enzyme in the carotenoid biosynthetic pathway and could catalyse prolycopene to lycopene that is a major part of total carotenoids (Pinheiro *et al*., 2019). In Arabidopsis (Park *et al*., 2002) and tomato (Isaacson *et al*., 2002), the loss-of-function of *CRTISO* influenced the accumulation of prolycopene, which delays the greening of Arabidopsis and changes the tomato fruit colour from red to orange. In addition to its aesthetic effect, *CRTISO* also has a major functional effect on photosynthetic efficiency. In the *ccr2* (*Atcrtiso*) mutants of Arabidopsis, chlorophyll accumulation during photomorphogenesis was significantly reduced (Park *et al*., 2002). *BoaCRTISO*-silenced plants have significantly decreased the levels of carotenoids and chlorophyll due to down-regulation of most carotenoids and chlorophyll biosynthesis genes (Jiang *et al*., 2021). In addition, carotenoid content and photosynthetic pigments were accumulated by various phytohormones (Divya *et al*., 2018). JA treatment could increase chlorophyll and carotenoid accumulation (Poonam *et al*., 2013). The role of JA regulating carotenoid in tomato revealed that the lycopene content was significantly decreased in JA-deficient mutants (*def1*) (Liu *et al*., 2012). Some studies have reported that JA was positively related to chlorophyll a and carotenoid contents, which are the key determinants of photosynthetic efficiency (Cotado *et al*., 2018; Sirhindi *et al*., 2020). In contrast, ABA was shown to limit photosynthetic capacity by reducing CO_2 assimilation and inactivating RuBisCo, which promotes stomatal closure (Seemann and Sharkey, 1987).

Fibrillins (FBNs), generally described as plastid lipid-associated proteins (PAPs), are the most abundant plastidial proteins. FBNs constitute a large protein family in photosynthetic organisms (Laizet *et al*., 2004). The first identified FBN in bell pepper was involved in carotenoid storage in chromoplasts (Deruère *et al*., 1994). In *Arabidopsis*, FBN1 and FBN2 proteins were involved in JA biosynthesis by interacting with enzymes like allene oxide synthase (AOS) catalysing the first step of JA synthesis (Torres-Romero *et al*., 2021). PAP6 is a member of fibrillin that is a homologue to FBN4 of *Arabidopsis* (Singh *et al*., 2010). Up to date, the specific function of FBN4 is still unknown, but many evidences support that PAP6 is involved in jasmonic acid accumulation.

This study identified a major QTL for grain length in hexaploid wheat. A candidate gene, *TaGL1-B1* encoding carotenoid isomerase, was isolated through multiple strategies. We revealed that *TaGL1-B1* positively regulates grain length and yield by EMS mutants and overexpression. We further found that a JA-mediated protein TaPAP6 strongly interacted with TaGL-B1. Transcriptome assays revealed that *TaPAP6* was involved in the regulation of JA. As yield improvement is a long-term primary breeding objective in common wheat, the *TaGL1-B1* we identified in this work provided a valuable information for improving wheat yield potential.

Results

Identification of *TaGL1-B1* regulating wheat grain length

Linkage mapping for grain length (GL) in a RIL (recombinant inbred lines) population UC1110/PI610750 (UP-RIL) revealed two stable QTLs on chromosome 1B. The *Qgl1.hau.1B* was flanked by markers *Wpt-5279* and *wPt-1251* with a phenotypic variance explained (PVE) of 7.67%–14.45% over the consecutive 3 years (Figure 1a; Table S1). The *Qgl2.hau.1B* locus was flanked by markers *wPt-9508* and *Id031* with a PVE of 9.59%–12.28% (Table S1). As *Qgl1.hau.1B* showed the relatively high PVE and LOD values, we mainly focused on this QTL for further analysis in this study. Genes annotation in the genome of Chinese Spring showed that the *Qgl1.hau.1B* (87.97–95.50 Mb) covered 50 putative annotated genes (Table S2). Based on genome resequencing and Sanger sequencing of two parents, 43 of the 50 candidate genes showed polymorphism between PI610750 and UC1110, and these polymorphic sites were subsequently used to develop 43 gene markers.

To fine map the *Qgl1.hau.1B*, a secondary F_2 population consisting of 5000 plants derived from PI610750 and UC1110 was genotyped using four flanking markers *wPt-5279/wPt-1251* (*Qgl1.hau.1B*) and *wPt-9508/Id031* (*Qgl2.hau.1B*). As a result, we identified 1206 F_2 plants without the *Qgl2.hau.1B*. To clone the *Qgl1.hau.1B*, 300 of the 1206 plants with extremely long grains and extremely short grains were planted to generate $F_{2:3}$ lines. Moreover, 48 lines with extremely long grains and 48 lines with extremely short grains in F_2 and $F_{2:3}$ lines were randomly selected to genotype by the 43 gene markers. Results showed that 10 gene markers clustering into a 0.98-Mb physical interval showed co-segregation with grain length (Figure 1b,c; Table S3). Analysis of expression levels retrieved from WheatOmics database (http://202.194.139.32/) showed that only *TraesCS1B02G090300* of the 10 genes was highly expressed in grain (Figure 1d; Table S4). Sequencing results revealed that *TraesCS1B02G090300* annotated as prolycopene isomerase showed multiple variants at the amino acid level and in the promotor region between two parents (Figure 1e). Therefore, we selected *TraesCS1B02G090300* as a candidate gene for *QGL.hau-1B* and named it as *TaGL1-B1*. Based on a 97-bp InDel (insertion/deletion) in the 9th intron of *TaGL1-B1*, we developed marker *Ta90300* to distinguish two alleles in UC1110 (designated *TaGL1-B1a*) and PI610750 (designated *TaGL1-B1b*) since this InDel was completely linked with other variant sites in the offspring of UP-RIL (Figure S1). *TaGL1-B1b* conferring long grain length (Figure 1f) was regarded as a superior allele for further analysis.

Re-running linkage mapping after adding *Ta90300* in the UP-RIL showed that the *QGL.hau-1B* was located between *Ta90300* and *Wpt-5279/wPt-1251* (Figure 1g) with a PVE of 13.07%–20.54% **(**Table S5). To verify the effect of *TaGL1-B1* in a natural population, we used *Ta90300* to identify 243 wheat accessions previously genotyped using the Wheat 660 K SNP array (Yang *et al*., 2019). GWAS results showed that *Ta90300* presented the highest significance level across all chromosomes (Figure 1h). The *t*-test showed that wheat accessions with *TaGL1-B1b* exhibited a significantly longer grain length than those with *TaGL1-B1a* over 3 years (Figure 1i).

EMS mutants and overexpression revealed the important role of *TaGL1* modulating wheat grain length

To verify the role of *TaGL1*, we screened four mutants (K2032 and K3215 with a premature stop codon of *TaGL1-A1*; K2309 and K329 with a splice region variant of *TaGL1-B1*) in the EMS-mutagenized tetraploid wheat Kronos mutant library (Figure 2a; Table S6). Phenotypic analysis showed that grain lengths of *TaGL1-A1* and *TaGL1-B1* mutant lines were decreased by 10.60% and 11.74% in the field, respectively, compared with

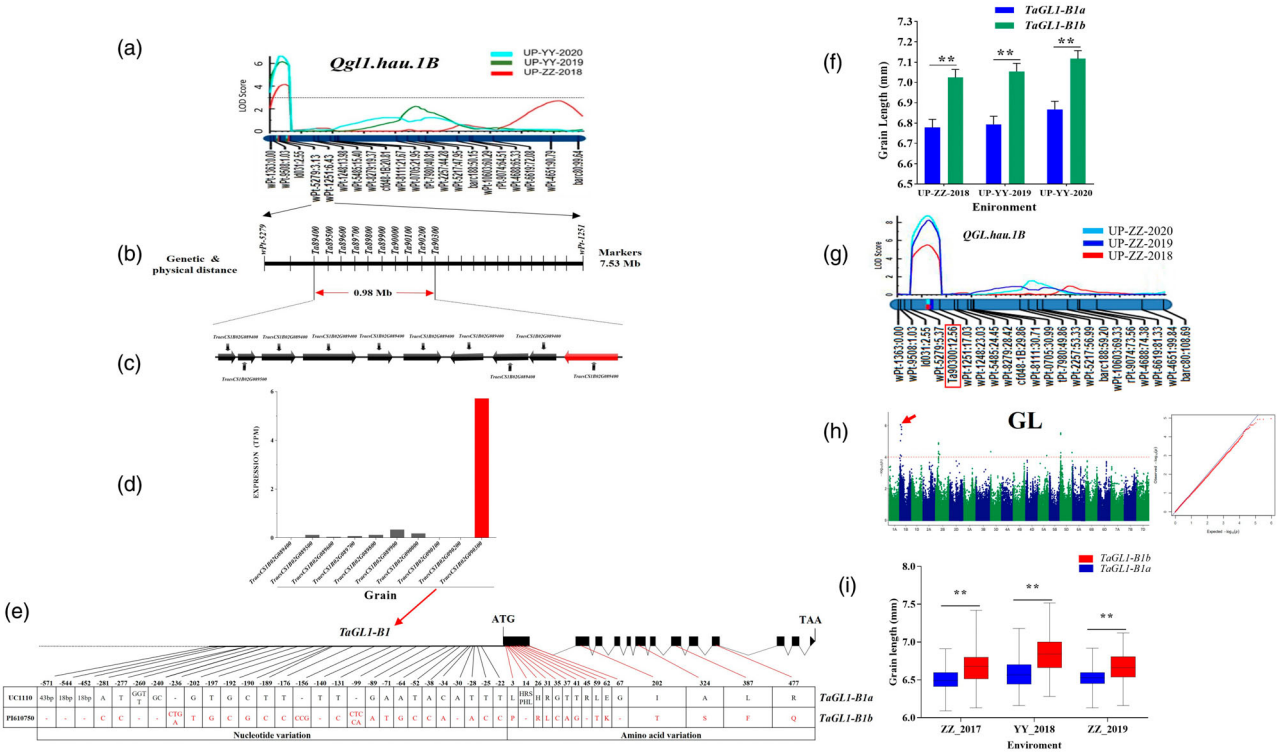

Figure 1 Identification and association of *TaGL1-B1* with grain length in wheat. (a) Linkage map of the *Qgl1.hau.1B* locus for grain length in the UC1110/PI610750 recombinant inbred lines (RIL) population. Horizontal dotted line represents a limit of detection (LOD) threshold value of 3.0. (b) Fine mapping of *Qgl.hau.1B* using F_2 and $F_{2:3}$ individuals revealed a 0.98-Mb cluster composed of 10 gene markers showing co-segregation with grain length. (c) Annotated genes in the target region of *Qgl1.hau.1B*. (d) Expression profiles of the 10 genes in grain. (e) Gene structure and protein variation of *TaGL1.B1* between UC1110 and PI610750. Black boxes and lines represent exons and introns, respectively. (f) Comparison of grain length between *TaGL1-B1a* and *TaGL1-B1b* alleles in UP-RIL. (g) Re-mapping QTL after adding the *TaGL1-B1* marker for wheat grain length. *Ta90300* was a marker for *TaGL1-B1*. (h) Manhattan and QQ plots of grain length identified by GWAS. Red arrow represents the *Ta90300* marker. GL, grain length. (i) Comparison of grain length between *TaGL1-B1a* and *TaGL1-B1b* alleles in the tested 243 accessions. Bars indicate means ± SEM, **: $P < 0.01$.

the wild-type Kronos (Figure 2b,d). But no significant difference was observed in grain width (GWD) between mutants and wild type except for K3215 (Figure 2c). Additionally, thousand grain weights (TGW) of *TaGL1-A1* and *TaGL1-B1* mutant lines were decreased by 36.53% and 16.33%, respectively (Figure 2e). The above data suggested that mutants of *TaGL1* in both A and B genomes had reduced grain length.

Furthermore, we constructed an overexpression vector containing cDNA of *TaGL1-B1b* from PI610750 and transferred it into the hexaploid wheat Fielder (*TaGL-B1a*). Three *TaGL1*-overexpressed positive lines were detected for expression level by qRT-PCR (Figure 2h) in the T_0 and T_1 generations, respectively, and were further self-crossed into the T_2 generation. Investigation of grain size after normal harvest in the field revealed that three independent *TaGL1*-overexpressed (*TaGL1*-OE) transgenic lines significantly increased grain length by 10.14% and TGW by 12.40% (Figure 2f–j) but had no significant difference for GWD compared to wild type (Figure 2g). It suggested that *TaGL1* positively regulated wheat grain length and thereby changed TGW.

TaGL1-B1 strongly interacted with TaPAP6

To further dissect the regulatory mechanism for grain length, we used the cDNA of *TaGL1-B1* as a bait to screen interaction proteins in the wheat cDNA library using yeast two-hybrid (Y2-H). A client, *TaPAP6* (fibrillin_dom) (Accession no. LS480641), was selected as it was possibly involved in jasmonic acid (JA) regulation (Youssef *et al.*, 2010). The interaction was further confirmed in the yeast cell by the Y-2H and tobacco leaf by Split Luciferase Complementation Assay (Figure 3a,b). Protoplast localization indicated that both TaGL1-B1 and TaPAP6 proteins were localized in the chloroplast (Figure 3c). qRT-PCR assay in flag leaves and seeds of *TaGL1-B1*-OE lines (Figure 3d; Figure S5) showed that the expression level of *TaPAP6* increased by approximately threefolds compared with WT. These results suggested that *TaGL1-B1* possibly affected the expression of *TaPAP6*.

Overexpression of *TaPAP6* significantly increased wheat grain length

To verify the function of *TaPAP6* regulating grain length, we constructed an overexpression vector containing *TaPAP6* and transferred it into the Fielder. *TaPAP6*-overexpressed positive lines were detected for expression level by qRT-PCR in T_0 and T_1 generations, respectively. Three independently *TaPAP6*-overexpressed lines with high expression level (Figure 3g) were further self-crossed into the T_2 generation. Investigation of grain size after normal harvest in the field indicated that the *TaPAP6*-overexpressed (*TaPAP6*-OE) lines significantly increased grain length by an average of 13.33% and TGW by an average of

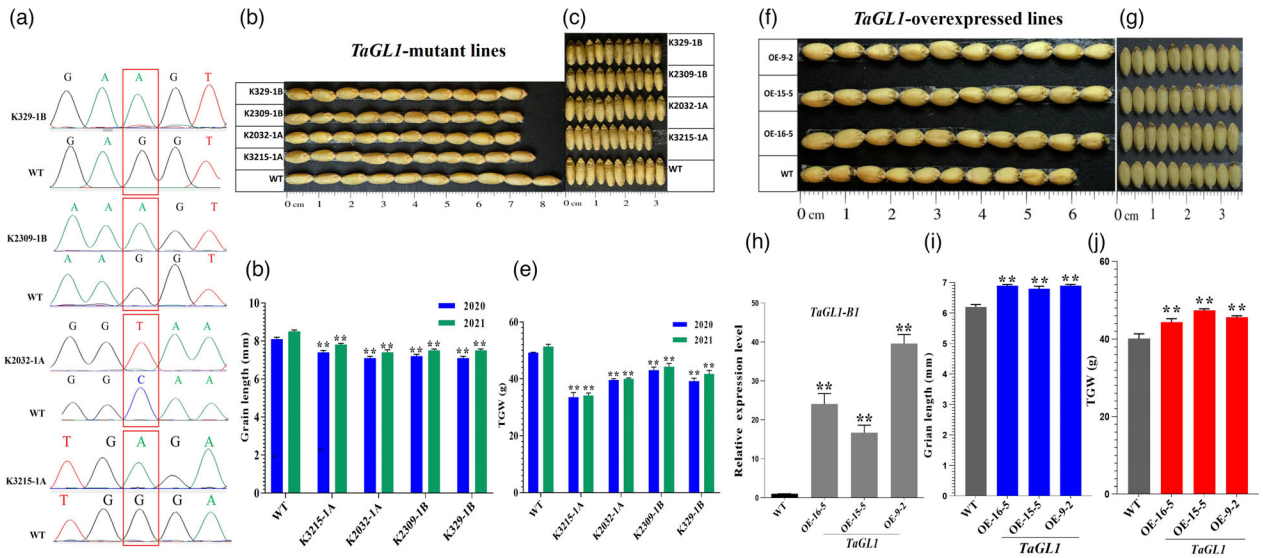

Figure 2 Functional verification of *TaGL1-B1* regulating grain length. (a) Mutation sites identified by sequencing. (b, d) Comparison of grain length between WT and *TaGL1* mutants. (c) Comparison of grain width between WT and *TaGL1* mutants. (e) Comparison of thousand-grain weight between WT and *TaGL1* mutants. (f, g, i, j) Comparison of grain length and grain width between WT and three *TaGL1*-overexpressed lines with high expression levels. (h) Relative expression level of three *TaGL1*-overexpressed lines. Bars indicate means ± SEM, **: $P < 0.01$.

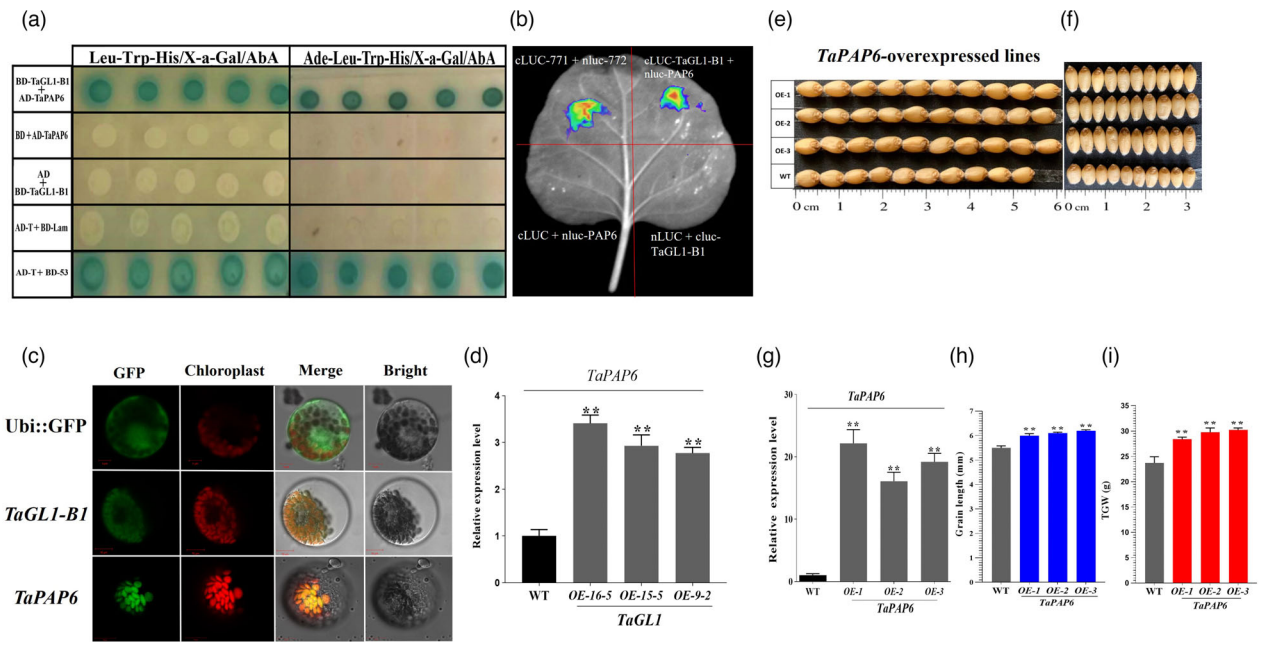

Figure 3 Interactions between *TaGL1-B1* and TaPAP6 proteins, and functional verification of *TaPAP6* regulating grain length. (a) Yeast two-hybrid assay showed the interaction between *TaGL1-B1* and TaPAP6. The transformants were plated on synthetically defined (SD) medium lacking Leu, Trp and histidine (His) but containing X-α-Gal/AbA (SD/-Leu/-Trp/-His/X-α-Gal) and on SD/-Leu/-Trp/-His/X-α-Gal medium lacking adenine (SD/-Leu/-Trp/-His/-Ade/X-α-Gal. X-α-Gal/AbA). Positive interaction was indicated by the presence of blue colonies. (b) Luciferase complementation assay in tobacco (*N. benthamiana*). The co-infiltration of cLUC-*TaGL1-B1* and nLUC-TaPAP6 resulted in luminescence generated by the complementation luciferase. cLUC-771 + nluc-772 was used as positive control. (c) Subcellular localization of *TaGL1-B1* and TaPAP6 in wheat protoplasts. GFP fusion with *TaGL1-B1* and GFP fusion with TaPAP6 under the control of the CaMV 35 S promoter were transiently expressed in wheat protoplasts. Bar = 10 μm. (d) Relative expression levels of *TaPAP6* in three *TaGL1-B1* overexpressed lines. (e) Comparison of grain length between WT and three *TaPAP6*-overexpressed lines. (f) Comparison of grain width between WT and *TaPAP6*-overexpressed lines. (g) Relative expression level of *TaPAP6* in three *TaPAP6*-overexpressed lines. (h) Grain length comparison between WT and three *TaPAP6*-overexpressed lines. (i) Comparison of thousand-grain weight between WT and *TaPAP6*-overexpressed lines. Bars indicate means ± SEM, **: $P < 0.01$.

13.94% but had no significant difference in GWD compared to wild type (Figure 3e,f,h,i). These results suggest that *TaPAP6* positively regulated wheat grain length.

TaPAP6 possibly contributed to the accumulation of jasmonic acid and suppression of ABA in wheat grains

As a member of the fibrillin family, *PAP6* was possibly involved in jasmonic acid (JA) regulation (Singh and McNellis, 2011; Youssef *et al*., 2010). Therefore, we performed transcriptome sequencing of *TaPAP6*-OE and WT lines to illustrate the association of *TaPAP6* with JA (Figure 4a). RNA-seq assay in *TaPAP6*-OE lines identified three sharply suppressed *JAR1* (jasmonic acid-amino synthetase) genes (Table S7) that primarily synthesize jasmonoyl-isoleucine (JA-Ile) by degradation of JA in KEGG (map04075 in https://www.kegg.jp/) analysis. However, five genes for JA synthesis were significantly up-regulated (Figure 4b; Table S9), including acyl-coenzyme A oxidase (ACX) that is essential for JA biosynthesis (Schilmiller *et al*., 2007). Therefore, we speculated that suppression of *JAR1* and up-regulation of JA biosynthetic genes by the improved expression of *TaPAP6* possibly resulted in the accumulation of JA. qRT-PCR further confirmed the expression change of JA-related genes in leaves of *TaPAP6*-OE (Figure S4).

To validate the hypothesis, we measured the JA content in seeds and leaves in overexpression and mutant lines. Results showed the JA content in *TaPAP6*-OE lines was significantly increased by 36.23% compared with wild-type Fielder (Figure 4d; Figure S2C). The JA content in *TaGL1*-OE lines was significantly increased by 27.31% (Figure 4c; Figure S2A) compared with wild-type Fielder, but was significantly decreased by 13.12%–24.42% in *TaGL1* mutants compared with wild-type Kronos (Figure 4e; Figure S2B).

A negative correlation was suggested between JA and ABA biosynthesis in wheat (Chen *et al*., 2020). To be consistent, two ABA synthetic key genes including abscisic-aldehyde oxidase (*AAO3.1* and *AAO3.2*) were significantly down-regulated in the *TaPAP6*-OE lines by RNA-seq assay (Figure 4b; Table S12). qRT-PCR further confirmed the expression changes of ABA-related genes in leaves of *TaPAP6*-OE (Figure S4). Determination results indicated that the ABA content showed a significant reduction of 13.11% in *TaGL1*-OE and 9.67% in *TaPAP6*-OE (Figure 4f,g; Figure S2D,F), respectively, compared with wild-type Fielder. On the contrary, the ABA content was increased in EMS mutant lines of *TaGL1* by 16.22%–22.14% compared with wild-type Kronos (Figure 4h; Figure S2E). These results revealed a negative correlation between JA and ABA. Collectively, *TaGL1* enhances grain length, possibly by modulating *TaPAP6* for concomitant control of JA and ABA.

Association of *TaGL1-B1* with carotenoid content in wheat grains

TaGL1-B1 showed a significant association with carotenoid content in wheat grains

Since *TaGL1-B1* was annotated as a carotenoid isomerase (*CRTISO*) involved in controlling carotenoid content (CC) in different plants (Isaacson *et al*., 2002; Jiang *et al*., 2021), we measured CC and carried out the linkage mapping in the UP-RIL. Results indicated that seven QTL were detected on 1B, 2A, 4B, 5B, 5D, 6A and 7A, whereas *Qcc.hau-1B* between *Ta90300* and *wPt-5279/wPt-1251* was the most stable QTL in all environments

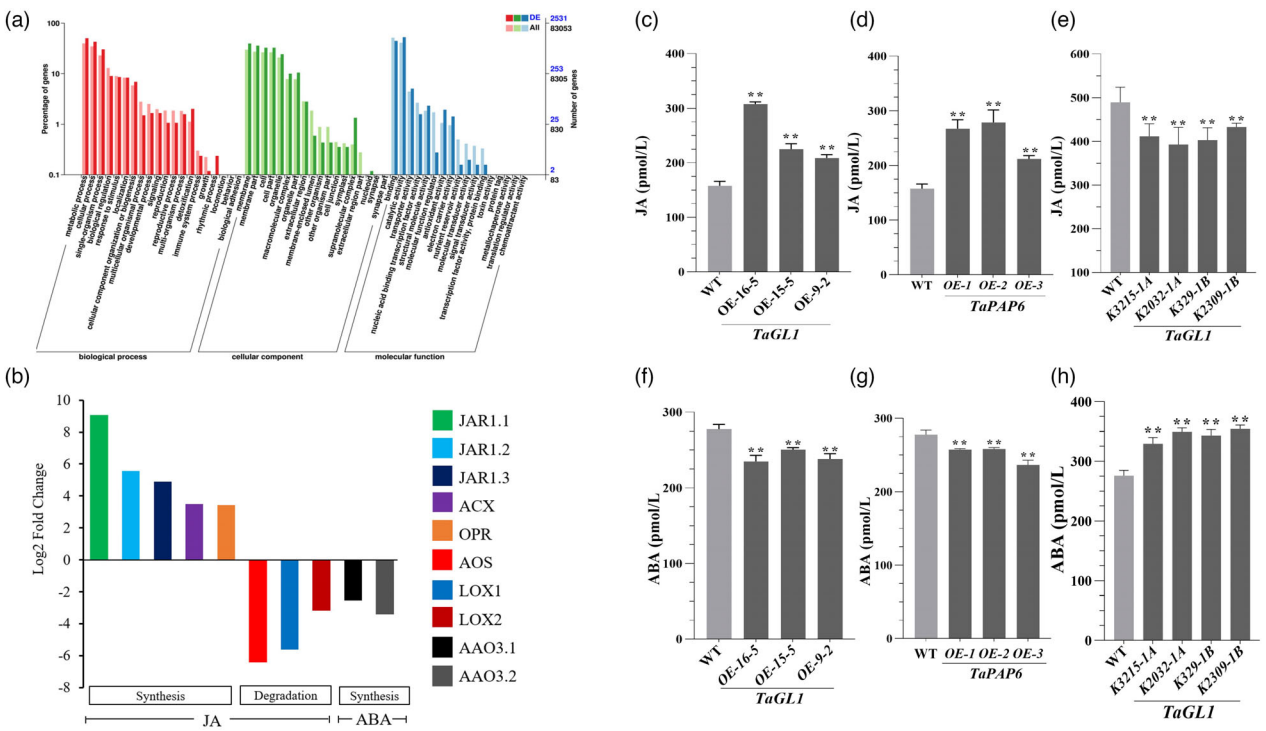

Figure 4 RNA-Seq analysis and hormone quantification. (a) Gene Ontology (GO) analysis of differentially expressed genes (DEG) between *TaPAP6*-OE and WT by RNA-seq. (b) DEGs involved in plant hormone metabolism. (c) Comparison of JA content in WT and *TaGL1*-OE. (d) Comparison of JA content in WT and *TaPAP6*-OE. (e) Comparison of JA content in WT and *TaGL1*-mutants. (f) Comparison of ABA content in WT and *TaGL1*-OE. (g) Comparison of ABA content in WT and *TaPAP6*-OE. (h) Comparison of ABA content in WT and *TaGL1*-mutants. Bars indicate means ± SEM, **: $P < 0.01$.

(Figure 5a) with a PVE of 15.10%–22.55% (Table S8). The *TaGL1-B1b* conferred a significantly higher CC than *TaGL1-B1a* (Figure 5b).

To analyse the association of *TaGL1-B1* with CC in a natural population, we performed GWAS in the 243 wheat accessions using the Wheat 660 K array covering *Ta90300*. Results detected 186 significant SNPs in three environments, but *Ta90300* was the most significant across all chromosomes (Figure 5c). Moreover, wheat varieties with *TaGL1-B1b* exhibited a significantly higher CC than those with *TaGL1-B1a* in all six replications over two years (Figure 5d).

Mutant and overexpression revealed the key role of TaGL1-B1 regulating wheat carotenoid and chlorophyll contents

In previous studies, the role of *TaGL1-B1* (*CRTISO*) regulating CC was validated in tomato, rice and *Arabidopsis* (Fang *et al.*, 2008; Isaacson *et al.*, 2002; Park *et al.*, 2002). Measurement results indicated that the CC was decreased by 8.32% in *TaGL1-A1* mutants and 12.91% in *TaGL1-B1* mutants compared with the wild-type Kronos (Figure 5e). Measurement of CC in overexpression lines indicated that the *CC was increased by 18.88% in TaGL1-OE lines* (Figure 5f) and by 15.31% in *TaPAP6*-OE lines compared with wild-type Fielder (Figure 5g).

Carotenoids play an important role in photosynthesis (Simkin *et al.*, 2015; Timm *et al.*, 2015) as carotenoids (e.g. *β*-carotene and xanthophylls) are key components of photosynthetic membranes (Sun *et al.*, 2018). Measurement results indicated that the chlorophyll content in mutants of *TaGL1-A1* and *TaGL1-B1* was decreased by 8.32% and 12.91%, respectively, compared with the wild-type Kronos (Figure 5h). However, the chlorophyll content was increased by 18.51% in *TaGL1-OE* lines (Figure 5i) and by 10.56% in *TaPAP6-OE* lines compared with wild-type Fielder (Figure 5j). These results suggest that *TaGL1* plays a key role in modulating photosynthesis of wheat plants, possibly through regulating carotenoid content.

The effect of *TaGL1-B1* on wheat yield

To evaluate the effect of *TaGL1-B1* on yield, we investigated grain yield of *TaGL1* overexpression and mutant lines in the field, respectively. *TaGL1-B1*-OE significantly enhanced yield per plant by 26.58% compared to wild-type Fielder (Figure 6a) over 2 years. The yield per plot (1 m^2) of three *TaGL1*-OE lines in the $T_{2:3}$ generation was significantly increased by 11.46% in Yuanyang (YY) and 10.63% in Zhengzhou (ZZ), respectively (Figure 6b), whereas the yield per plot of *TaGL1-A1* and *TaGL1-B1* mutants was significantly decreased by 71.36% and 45.57% in Yuanyang and was decreased by 57.47% and 28.38% in Zhengzhou, respectively, compared with the wild-type Kronos (Figure 6c). To identify the association of *TaGL1-B1* alleles with yield in a natural population, we also investigated the yield per

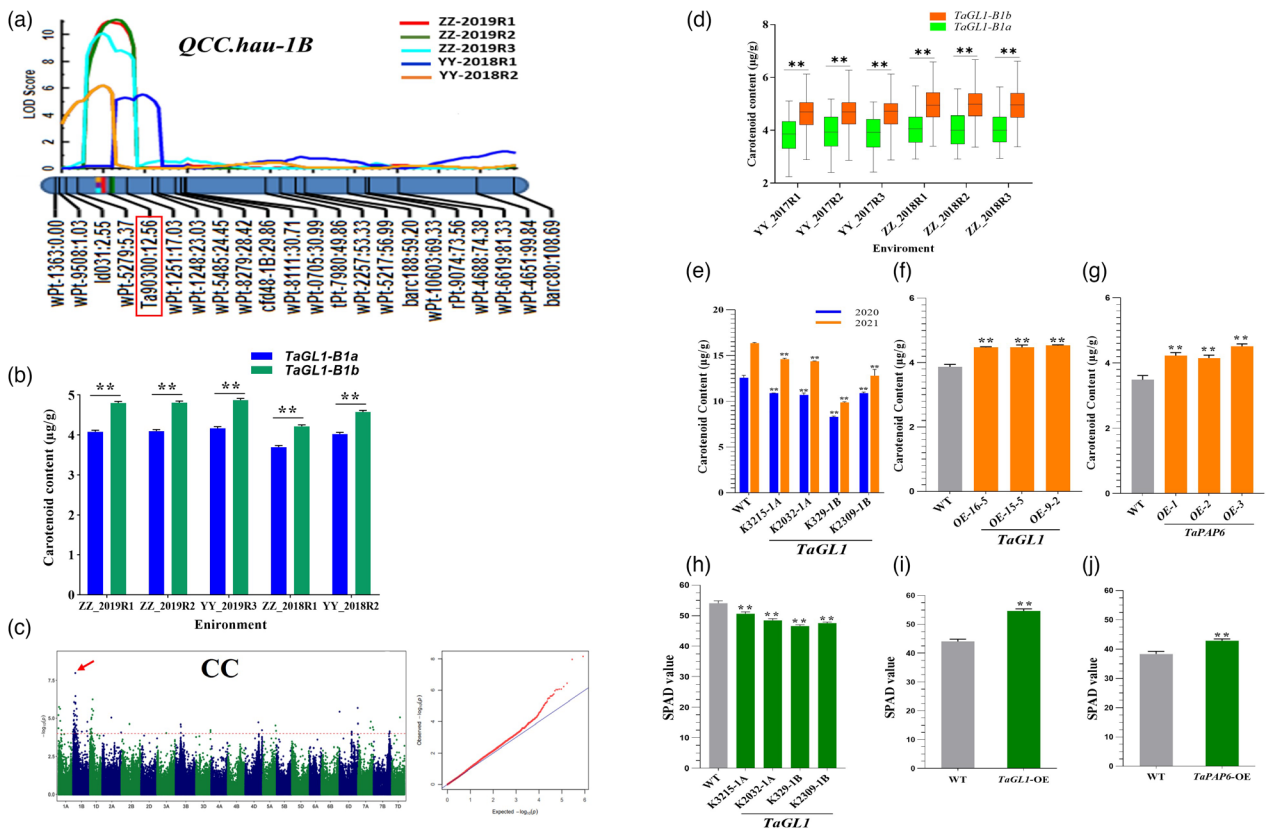

Figure 5 Association of *TaGL1-B1* with carotenoid content. (a) Validation of association of *TaGL1-B1* with wheat grain carotenoid content by QTL re-analysis. *Ta90300* was a putative marker for *TaGL1-B1*. (b) Comparison of carotenoid content between wheat lines with *TaGL1-B1a* and *TaGL1-B1b* in UP-RIL. (c) Manhattan and QQ plots of grain length identified by GWAS. Red arrow represents the *Ta90300* marker. CC, carotenoid content. (d) Comparison of carotenoid content (μg/g) between *TaGL1-B1a* and *TaGL1-B1b*. (e) Comparison of CC between WT and *TaGL1*-mutants. (f) Comparison of CC between WT and *TaGL1-OE*. (g) Comparison of CC between WT and TaPAP6-OE. (h, i, j) Comparison chlorophyll contents between WT and *TaGL1* mutants, WT and *TaGL1-OE*, WT and *TaPAP6*, respectively. Bars indicate means ± SEM, **: $P < 0.01$.

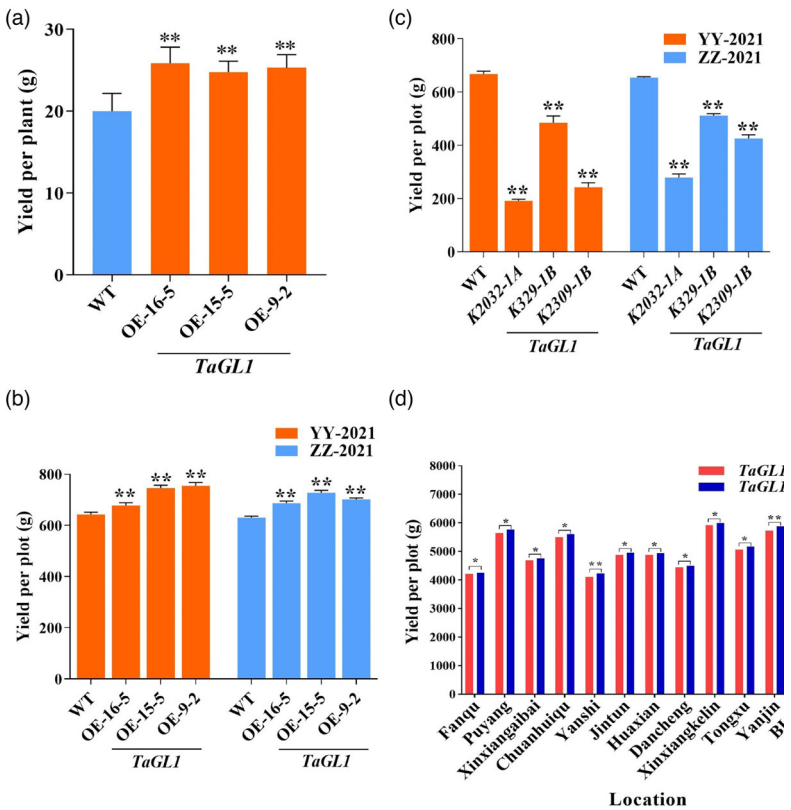

Figure 6 The effect of *TaGL1-B1* on wheat yield. (a) Comparison of average yield per plant between WT and *TaGL1-OE* in T_2 and T_3. (b) Comparison of yield per plot between WT and *TaGL1-OE* in $T_{2:3}$ at Zhengzhou (ZZ) and Yuanyang (YY). (c) Comparison of grain yield per plot between WT and *TaGL1*-mutants at Zhengzhou (ZZ) and Yuanyang (YY). (d) Comparison of average yield per plot of the 243 accessions with *TaGL1-B1a* and *TaGL1-B1b* alleles at 11 locations. Bars indicate means ± SEM, *: $P < 0.05$; **: $P < 0.01$.

plot (12.8 m^2) of 243 wheat accessions with three replications. Results indicated that varieties with *TaGL1-B1b* showed a significantly higher yield per plot by a range of 0.80%–2.81% than those with *TaGL-B1a* in 11 locations (Figure 6d).

Based on our findings and previous studies, we proposed *TaGL1-TaPAP6* mediating wheat grain size and yield. *TaGL1* positively contributes to the expression of *TaPAP6* and thereby results in the accumulation of JA and suppression of ABA synthesis. JA was involved in enhanced carotenoids (Cotado *et al.*, 2018; Sirhindi *et al.*, 2020). Together, an increase in carotenoid and a decrease in ABA could boost photosynthesis, which provides a pool energy source for grain size and yield. As a result, the overexpression of the *TaGL1-B1* showed a definite increase in wheat yield.

Discussion

Grain size is one of the most important agronomic traits determining wheat yield and is controlled by several genetic factors. In recent years, grain-related traits have received widespread attention in molecular genetics. Various critical biological mechanisms, including ubiquitination, phytohormones, G-proteins and photosynthesis, have been reported to be involved in grain size (Liu *et al.*, 2018; Pan *et al.*, 2018). Previous studies demonstrated that *CRTISO* played an important role in photosynthetic efficiency and plant growth by accumulating chlorophyll (Park *et al.*, 2002). Previous reports showed that *crtiso* mutants exhibit decreased levels of carotenoids and chlorophyll in Chinese Kale (Sun *et al.*, 2020) and rice (Chai *et al.*, 2011), implying that *CRTISO* possessed a deleterious impact on photosynthesis. In the present study, we identified the *TaGL1-B1* (*CRTISO*) positively regulating wheat grain length. We also found that *TaGL1-B1* regulated carotenoid contents possibly through the change of JA level, thereby effected photosynthesis which probably led to the alteration of grain size. Therefore, we proposed that JA, chlorophyll and carotenoid precursors might be key components of a coordinated signal network regulating wheat grain size during photosynthesis.

To further understand the mechanism of *TaGL1-B1* controlling grain length, we screened its interaction protein by Y2-H and identified the PAP6 (also known as fibrillin) that is required for plastoglobule development (Singh *et al.*, 2010; Vidi *et al.*, 2007; Ytterberg *et al.*, 2006). Plastoglobules are thylakoid-attached lipoprotein structure to store lipids including antioxidants such as tocopherols, carotenes and plastoquinones (Austin *et al.*, 2006; Tevini and Steinmüller, 1985). Since plastoglobules include the enzyme Allene oxide synthase (AOS), which is responsible for the synthesis of the jasmonate precursor 12-oxophytodienoic acid (OPDA), it is possible that plastoglobules are involved in jasmonate synthesis as well (Oliw and Hamberg, 2017). During low-temperature and photooxidative stress, a subfamily (FIB1a, FIB1b and FIB2) of *Arabidopsis* fibrillins was reported to regulate jasmonate synthesis (Singh *et al.*, 2010). In addition, OsFBN1 participates in the development of plastoglobules and the metabolism of lipids in chloroplasts, and they coordinately govern the development and grain filling (Li *et al.*, 2019). Several evidences suggested that FBN might be involved in JA accumulation by regulating plastoglobules content.

In the present study, *TaPAP6* caused alterations in the expression of several genes required to produce various hormones, including JA and ABA, in seeds and leaves. In tomato, the

particular role of JA-inducible genes and jasmonates in flower and seed development was found (Wasternack *et al.*, 2013). In metabolite analyses, JA showed an apparent increase in both leaves and seeds of overexpression lines, whereas significant decrease in ABA was detected. On the contrary, a reverse pattern of JA and ABA contents was observed in mutants of *TaGL1* gene. JA influenced photosynthesis and antioxidants in plants by modulating their protein profiles (Maserti *et al.*, 2011). The expression of the JA-inducible genes *ACX*, *OPR* and *AOS* was increased in *TaPAP6* overexpression lines, most likely as a result of the increased JA content. The previous reports demonstrated the possible contribution of JA synthetic genes in endosperm development (Dave *et al.*, 2011). Furthermore, the influence of JA on grain weight has been studied using a JA synthesis gene mutant *tgw1*, which generates smaller grains with less JA in wheat (Chen *et al.*, 2020). Nevertheless, the potential role of JA in regulating grain size remains obscure.

Based on this work and previous reports, we proposed that *TaGL1-TaPAP6* control grain length in wheat. However, more experimental work is required to illustrate the regulatory mechanism underpinning JA-mediated morphogenesis to yield formation. Finally, our study demonstrates that *TaGL1-B1* and *TaPAP6* work together to favourably control grain length and carotenoids. Therefore, *TaGL1-B1* and *TaPAP6* are useful for pyramiding breeding in view of improving yield and also provide a new insight into further understanding of JA influencing wheat grain development. With the improvement of grain size, a drop in grain number per spike or other unfavourable phenotypes was frequently observed, which thereby caused no significant change or even decrease of wheat yield. However, the expression of *TaGL1*-OE contributed a high yield, suggesting that the *TaGL1* gene showed a great potential to improve wheat yield.

Material and methods

Plant materials and phenotyping

A bi-parental F_{10} recombinant inbred lines (RIL) population with 187 lines, developed from UC111 with small grain size and PI610750 with large grain size (UP-RIL), was planted at Zhengzhou (34.87° N, 115.59° E) in 2018 (ZZ-2018) and at Yuanyang (35.05° N, 113.97° E) in 2019 (YY-2019) and 2020 (YY-2020). A secondary F_2 population containing 5000 plants was generated from a cross of UC1110 and PI610750, and a derivative $F_{2:3}$ population containing 300 lines with extreme phenotype was selected for fine mapping of the target QTL. An association panel composed of 243 accessions was planted in Zhengzhou and Yuanyang during the 2017–2020 cropping seasons, respectively. Each line was planted with two replications. Each plot contained 12 rows with the 1.5m length and 3.1m width. All test materials grew well, and no lodging occurred in the field. After harvesting, grain length was measured using the SeedCounter SC 5000 (Australia). To determine the plot yield (1 m^2) of transgenic and mutant lines with their corresponding wild types, 50 seeds in each plot (1 m × 1 m) were planted in the field. To investigate plot yield (12.8 m^2) of the association panel, each accession was planted in a plot (3.2 m × 4 m) with three replications at 11 different locations, including Fanqu (33.66° N, 114.67° E), Puyang (35.80° N, 115.02° E), Xinxiangaibai (35.16° N, 113.81° E), Chuanhuiqu (33.65° N, 114.69° E), Yanshi (34.74° N, 112.78° E), Jintun (34.23° N, 115.12° E), Huaxian (35.58° N, 114.51° E), Dancheng (33.67° N, 115.19° E), Xinxiangkelin (35.32° N, 113.92° E), Tongxu (34.50° N, 114.47° E) and Yanjin (35.14° N, 114.23° E). Total grain weight was measured when the water content was below 14% after normal harvest.

Linkage mapping

The genetic linkage map was constructed using 1494 markers, including DArT, SSR and ESTs (Lowe *et al.*, 2011), by IciMapping V4.1 (http://www.isbreeding.net/). Marker allele frequency <0.3 or containing >10% missing data were rejected. The screened markers were binned based on the pattern of segregation in the UP-RIL using the BIN function of IciMapping 4.1 and ICIM-ADD model (Li *et al.*, 2007), and Kosambi function was used for the construction of genetic linkage map. Phenotypic variance explained (PVE) was used to evaluate QTL effect based on the ICIM-ADD model (Ren *et al.*, 2017). Default was used for parameter designs. The LOD scores for detecting significant QTL were calculated at the $P < 0.05$ level from 1000 permutations, and the threshold of LOD score was set to 3.0.

Resequencing genomes of UC1110 and PI610750

The young leaves of UC1110 and PI610750 were sampled for resequencing genomes by the Beijing Novogene Company. Genomic DNA was prepared using the Takara MiniBEST plant Genomic DNA Extraction Kit (9768, Takara, Dalian, China) and was sequenced using the Illumina Hiseq. More than 148 G (10 × genome size of hexaploidy wheat) clean reads were generated for each sample. Clean reads were mapped to IWGSC annotation V1.1 using BWA alignment software (0.7.8-r455) (Li and Durbin, 2009). The SAMTOOLS (0.1.19-44 428 cd) was used to detect SNPs, Indels (Li *et al.*, 2009), and the ANNOVAR (2013Aug23) was used to annotate the detected variations (Wang *et al.*, 2010).

Genotyping and genome-wide association study

The 243 wheat accessions were genotyped using the wheat 660 K SNP array (Yang *et al.*, 2019). SNPs with a minor allele frequency (MAF) >5% and a call rate >10% were used for further analysis. Quality control measures were applied to the genotype data using the PLINK software with thresholds of --maf 0.02 and --geno 0.1 (http://zzz.bwh.harvard.edu/plink/tutorial) (Purcell *et al.*, 2007). GWAS was performed using R software through the GAPIT package based on the mixed linear model (PCA + K) (Lipka *et al.*, 2012). The threshold (1.0 e-4) for *P*-value was calculated using a modified Bonferroni correction method (Genetic type 1 error calculator, v.0.2; Li *et al.*, 2013).

EMS mutants of the *TaGL1* gene

Seeds of the tetraploid wheat Kronos were mutagenized by the group of Jorge Dubcovsky from UC Davis using EMS. Four mutant lines (K2032 and K3215 with a premature stop codon of *TaGL1-A1*; K2309 and K329 with a splice region variant of *TaGL1-B1*) were screened and planted at Yuanyang during the 2019–2020 and 2020–2021 cropping seasons. All mutation sites were verified by sequencing (Table S7) and were further backcrossed for two times with wild type for further analysis.

Construct of overexpression lines

To produce *TaGL1*-OE and *TaPAP6*-OE plants, the CDSs of *TaGL1-B1* and *TaPAP6* were cloned into the wheat LGY-OE3 vector with the Ubi promoter. These vectors containing target genes were transformed by *Agrobacterium*-mediated infection into immature embryos of the hexaploid wheat variety Fielder to obtain the

TaGL1-OE and *TaPAP6*-OE lines. Positively T_0 transgenic plants detected by PCR were self-pollinated into T_1 and T_2 generations. Three independent lines of T_2 and $T_{2:3}$ plants with high expression levels by qRT-PCR were chosen to measure grain length, grain width, TGW, grain yield per plant, carotenoids, chlorophyll, JA and ABA.

qRT-PCR

Total RNA was extracted from seeds and leaves, respectively, using the RNAprep Pure Plant Kit (Tiangen, Beijing, China), and reverse transcribed into cDNA using Hifair II 1st Strand cDNA Synthesis Super Mix for qPCR (gDNA digester plus) (Yeasen, Shanghai, China) according to the manufacturer's instructions. qRT-PCR was performed using the Hieff qPCR SYBR Green Master Mix (Yeasen), and TaActin (GeneBank accession number: AB181991) was used as the internal control. Three biological replicates were performed for each experiment.

RNA sequencing analysis

Total RNA samples were prepared from mature seeds of wild-type Fielder and *TaPAP6*-OE lines with three biological replicates. Total RNA was extracted and sequenced by BMKCloud (Beijing, China). Additional detailed information was provided on the BMKCloud website (https://international.biocloud.net/). The expression profiles of *TaGL1-B1* and *TaPAP6* in different tissues were retrieved from WheatOmics (http://202.194.139.32/) and shown in Figure S6.

Yeast two-hybrid assay

The CDS of *TaGL1-B1* was amplified and subcloned into the bait plasmid pGBKT7 (Clontech, Mountain View, CA), and full-length CDS of *TaPAP6* was amplified and subcloned into the prey plasmid pGADT7 (Clontech). Yeast two-hybrid assays were performed after the co-transformation of both plasmids into *Saccharomyces cerevisiae* strain AH109 (Clontech) according to the manufacturer's instructions. The clones were dotted on selective plates and cultured at 30 °C for 3–5 days. The interaction between the expressed proteins was determined by the growth of the co-transformation on a selection medium (SD/−Trp/−Leu/-His/−Ade) following the Yeast Protocols Handbook (Takara Bio). Positive clones were expected to grow with blue colour.

Subcellular localization

The full-length CDSs of *TaGL1-B1* and *TaPAP6* were amplified and subcloned into the pJIT163-GFP vector. The verified fusion constructs and the control pJIT163-GFP vector were introduced into wheat mesophyll protoplasts using the PEG-mediated method as previously described (Liu *et al*., 2020). After a 16-h incubation, microscopic examination was done under 488- and 543-nm illumination using a Zeiss LSM700 microscope (ZEISS Germany).

Split luciferase complementation assay

The CDSs of *TaGL1-B1* and *TaPAP6* were inserted into pCAMBIA1300-cLUC and pCAMBIA1300-nLUC to form cLUC-TaGL1-B1 and nLUC-TaPAP6-B1, respectively. One-month leaves of *Nicotiana benthamiana* co-infiltrated with Agrobacterium expressing cLUC-TaGL1-B1 and nLUC-TaPAP6-B1. cLUC-TaGL1-B1 and nLUC, cLUC and nLUC-TaPAP6, and cLUC and nLUC were used as negative controls. The luminescence images were captured using a plant living imaging system (Berthold, Night Shade LB 985).

Determination of carotenoids, chlorophyll, JA and ABA

The method for determination of the carotenoid content in wheat grains was based on Approved Method 14–50 (AACC, 2000) with slight modification. Seeds from each test accession were ground into fine powder using a lab flour milling machine (Model No. JXFM110), and 8 g of flour was used to measure carotenoid from each sample. The extracts of carotenoid were measured using spectrophotometry with three replications as described in Beleggia *et al*. (2010).

The chlorophyll content of wheat plants was determined at the heading stage by the SPAD-502 meter (Konica Minolta, Japan). Ten SPAD values were recorded from the flag leaf of each accession. JA and ABA were determined by ELISA kits (Jianglai Biotechnology Co. Ltd., Shanghai, China) according to the manufacturer's instructions. The absorbance of the standard material at 450 nm was used to calculate the JA and ABA standard curves.

Acknowledgement

This work was funded by the National Natural Science Foundation (32072057 and U1804234), Henan Major Science and Technology Projects (201300110800 and 201300111600) and Key Scientific and Technological Project of Henan Province (222102110026) of China. The tetraploid wheat accessions were kindly provided by Prof. Daowen Wang from Henan Agricultural University.

Conflicts of interest

The authors declare no conflict of interest.

Author contributions

FC conceived the project and organized the manuscript. MN, GL, LZ, YZ, BZ, XY, AAY, LZ, ZD and SC performed QTL mapping, GWAS analysis, cloned and identified the function of *TaGL1* gene. MN, GL, LZ, YZ and BZ investigated agronomic traits. MN and FC wrote the manuscript.

References

AACC (American Association of Cereal Chemists), 2000. AACC Official Method 14-50. In: *Approved Methods of the American Association of Cereal Chemists*, tenth ed. AACC (American Association of Cereal Chemists), St. Paul, MN, USA.

Austin, J. R., Frost, E., Vidi, P.-A., Kessler, F., & Staehelin, L. A. (2006). Plastoglobules are lipoprotein subcompartments of the chloroplast that are permanently coupled to thylakoid membranes and contain biosynthetic enzymes. *Plant Cell*, **18**, 1693–1703.

Beleggia, R., Platani, C., Nigro, F. and Cattivelli, L. (2010) A micro-method for the determination of Yellow Pigment Content in durum wheat. *J. Cereal Sci.* **52**, 106–110.

Brinton, J., Simmonds, J., Minter, F., Leverington-Waite, M., Snape, J. and Uauy, C. (2017) Increased pericarp cell length underlies a major quantitative trait locus for grain weight in hexaploid wheat. *New Phytol.* **215**, 1026–1038.

Browse, J. (2009) Jasmonate passes muster: a receptor and targets for the defense hormone. *Annu. Rev. Plant Biol.* **60**, 183–205.

Chai, C., Fang, J., Liu, Y., Tong, H., Gong, Y., Wang, Y., Liu, M. *et al*. (2011) ZEBRA2, encoding a carotenoid isomerase, is involved in photoprotection in rice. *Plant Mol. Biol.* **75**, 211–221.

Che, R., Tong, H., Shi, B., Liu, Y., Fang, S., Liu, D., Xiao, Y. *et al*. (2016) Control of grain size and rice yield by *GL2*-mediated brassinosteroid responses. *Nat. Plants.* **2**, 15195.

Chen, Y., Yan, Y., Wu, T.-T., Zhang, G.-L., Yin, H., Chen, W., Wang, S. *et al*. (2020) Cloning of wheat keto-acyl thiolase 2B reveals a role of jasmonic acid in grain weight determination. *Nat. Commun.* **11**, 6266.

Cotado, A., Müller, M., Morales, M. and Munné-Bosch, S. (2018) Linking jasmonates with pigment accumulation and photoprotection in a high-mountain endemic plant, *Saxifraga longifolia*. *Environ. Exp. Bot.* **154**, 56–65.

Dave, A., Hernández, M.L., He, Z., Andriotis, V.M.E., Vaistij, F.E., Larson, T.R. and Graham, I.A. (2011) 12-oxo-phytodienoic acid accumulation during seed development represses seed germination in *Arabidopsis*. *Plant Cell* **23**, 583–599.

Deruère, J., Römer, S., d'Harlingue, A., Backhaus, R.A., Kuntz, M. and Camara, B. (1994) Fibril assembly and carotenoid overaccumulation in chromoplasts: a model for supramolecular lipoprotein structures. *Plant Cell* **6**, 119–133.

Divya, P., Puthusseri, B., Savanur, M.A., Lokesh, V. and Neelwarne, B. (2018) Effects of methyl jasmonate and carotenogenic inhibitors on gene expression and carotenoid accumulation in coriander (*Coriandrum sativum* L.) foliage. *Food Res. Int.* **111**, 11–19.

Fang, J., Chai, C., Qian, Q., Li, C., Tang, J., Sun, L., Huang, Z. *et al*. (2008) Mutations of genes in synthesis of the carotenoid precursors of ABA lead to pre-harvest sprouting and photo-oxidation in rice. *Plant J.* **54**, 177–189.

Guan, P., Lu, L., Jia, L., Kabir, M.R., Zhang, J., Lan, T., Zhao, Y. *et al*. (2018) Global QTL analysis identifies genomic regions on chromosomes 4A and 4B harboring stable loci for yield-related traits across different environments in wheat (*Triticum aestivum* L.). *Front. Plant Sci.* **9**, 529.

Guo, L., Ma, M., Wu, L., Zhou, M., Li, M., Wu, B., Li, L. *et al*. (2022) Modified expression of *TaCYP78A5* enhances grain weight with yield potential by accumulating auxin in wheat (*Triticum aestivum* L.). *Plant Biotechnol. J.* **20**, 168–182.

Guo, X., Fu, Y., Lee, Y.J., Chern, M., Li, M., Cheng, M., Dong, H. *et al*. (2022) The PGS1 basic helix-loop-helix protein regulates *Fl3* to impact seed growth and grain yield in cereals. *Plant Biotechnol. J.* **20**, 1311–1326.

Hou, J., Jiang, Q., Hao, C., Wang, Y., Zhang, H. and Zhang, X. (2014) Global selection on sucrose synthase haplotypes during a century of wheat breeding. *Plant Physiol.* **164**, 1918–1929.

Isaacson, T., Ronen, G., Zamir, D. and Hirschberg, J. (2002) Cloning of tangerine from tomato reveals a carotenoid isomerase essential for the production of β-carotene and xanthophylls in plants. *Plant Cell* **14**, 333–342.

Jiang, M., Zhang, F., Yuan, Q., Lin, P., Zheng, H., Liang, S., Jian, Y. *et al*. (2021) Characterization of *BoaCRTISO* reveals its role in carotenoid biosynthesis in Chinese Kale. *Front. Plant Sci.* **12**, 662684.

Laizet, Y., Pontier, D., Mache, R. and Kuntz, M. (2004) Subfamily organization and phylogenetic origin of genes encoding plastid lipid-associated proteins of the fibrillin type. *J. Genome Sci. Tech.* **3**, 19–28.

Li, H., Ye, G. and Wang, J. (2007) A Modified Algorithm for the Improvement of Composite Interval Mapping. *Genetics* **175**, 361–374.

Li, H., Handsaker, B., Wysoker, A., Fennell, T., Ruan, J., Homer, N., Marth, G. *et al*. (2009) The sequence Alignment/Map format and SAMtools. *Bioinformatics* **25**, 2078–2079.

Li, Y., Fan, C., Xing, Y., Jiang, Y., Luo, L., Sun, L., Shao, D. *et al*. (2011) Natural variation in *GS5* plays an important role in regulating grain size and yield in rice. *Nat. Genet.* **43**, 1266–1269.

Li, H., Peng, Z., Yang, X., Wang, W., Fu, J., Wang, J., Han, Y. et al. (2013). Genome-wide association study dissects the genetic architecture of oil biosynthesis in maize kernels. *Nat. Genet.* **45**, 43–50.

Li, J., Yang, J., Zhu, B. and Xie, G. (2019) Overexpressing OsFBN1 enhances plastoglobule formation, reduces grain-filling percent and jasmonate levels under heat stress in rice. *Plant Sci.* **285**, 230–238.

Lipka, A.E., Tian, F., Wang, Q., Peiffer, J., Li, M., Bradbury, P.J., Gore, M.A. *et al*. (2012) GAPIT: genome association and prediction integrated tool. *Bioinformatics* **28**, 2397–2399.

Liu, L., Wei, J., Zhang, M., Zhang, L., Li, C. and Wang, Q. (2012) Ethylene independent induction of lycopene biosynthesis in tomato fruits by jasmonates. *J. Exp. Bot.* **63**, 5751–5761.

Liu, J., Chen, J., Zheng, X., Wu, F., Lin, Q., Heng, Y., Tian, P. *et al*. (2017) *GW5* acts in the brassinosteroid signalling pathway to regulate grain width and weight in rice. *Nat. Plants* **3**, 17043.

Liu, Q., Han, R., Wu, K., Zhang, J., Ye, Y., Wang, S., Chen, J. *et al*. (2018) G-protein βγ subunits determine grain size through interaction with MADS-domain transcription factors in rice. *Nat. Comm.* **9**, 852.

Liu, H., Li, H., Hao, C., Wang, K., Wang, Y., Qin, L., An, D. *et al*. (2020) TaDA1, a conserved negative regulator of kernel size, has an additive effect with *TaGW2* in common wheat (*Triticum aestivum* L.). *Plant Biotechnol. J.* **18**, 1330–1342.

Lowe, I., Jankuloski, L., Chao, S., Chen, X., See, D. and Dubcovsky, J. (2011) Mapping and validation of QTL which confer partial resistance to broadly virulent post-2000 North American races of stripe rust in hexaploid wheat. *Theor. Appl. Genet.* **123**, 143–157.

Lyons, R., Manners, J.M. and Kazan, K. (2013) Jasmonate biosynthesis and signaling in monocots: a comparative overview. *Plant Cell Rep.* **32**, 815–827.

Ma, L., Li, T., Hao, C., Wang, Y., Chen, X. and Zhang, X. (2016) TaGS5-3A, a grain size gene selected during wheat improvement for larger kernel and yield. *Plant Biotechnol. J.* **14**, 1269–1280.

Maserti, B.E., Del Carratore, R., Croce, C.M.D., Podda, A., Migheli, Q., Froelicher, Y., Luro, F. *et al*. (2011) Comparative analysis of proteome changes induced by the two spotted spider mite *Tetranychus urticae* and methyl jasmonate in citrus leaves. *J. Plant Physiol.* **168**, 392–402.

Nadolska-Orczyk, A., Rajchel, I.K., Orczyk, W. and Gasparis, S. (2017) Major genes determining yield-related traits in wheat and barley. *Theor. Appl. Genet.* **130**, 1081–1098.

Oliw, E.H. and Hamberg, M. (2017) An allene oxide and 12-oxophytodienoic acid are key intermediates in jasmonic acid biosynthesis by *Fusarium oxysporum*. *J. Lipid Res.* **58**, 1670–1680.

Pan, J., Huang, D., Guo, Z., Kuang, Z., Zhang, H., Xie, X., Ma, Z. *et al*. (2018) Overexpression of microRNA408 enhances photosynthesis, growth, and seed yield in diverse plants: MiR408 promotes photosynthesis and grain yield. *J. Integr. Plant Biol.* **60**, 323–340.

Park, H., Kreunen, S.S., Cuttriss, A.J., DellaPenna, D. and Pogson, B.J. (2002) Identification of the carotenoid isomerase provides insight into carotenoid biosynthesis, prolamellar body formation, and photomorphogenesis. *Plant Cell* **14**, 321–332.

Pinheiro, T.T., Peres, L.E.P., Purgatto, E., Latado, R.R., Maniero, R.A., Martins, M.M. and Figueira, A. (2019) Citrus carotenoid isomerase gene characterization by complementation of the "Micro-Tom" tangerine mutant. *Plant Cell Rep.* **38**, 623–636.

Poonam, S., Kaur, H. and Geetika, S. (2013) Effect of jasmonic acid on photosynthetic pigments and stress markers in *Cajanus cajan* (L.) Millsp. seedlings under copper stress. *Am. J. Political Sci.* **04**, 817–823.

Purcell, S., Neale, B., Todd-Brown, K., Thomas, L., Ferreira, M.A.R., Bender, D., Maller, J. *et al*. (2007) PLINK: A Tool Set for Whole-Genome Association and Population-Based Linkage Analyses. *Am. J. Hum. Genet.* **81**, 559–575.

Ren, Y., Hou, W., Lan, C., Basnet, B. R., Singh, R. P., Zhu, W., Cheng, X. *et al*. (2017). QTL Analysis and Nested Association Mapping for Adult Plant Resistance to Powdery Mildew in Two Bread Wheat Populations. *Front. Plant Sci.* **8**, 1212.

Schilmiller, A.L., Koo, A.J.K. and Howe, G.A. (2007) Functional Diversification of Acyl-Coenzyme A Oxidases in Jasmonic Acid Biosynthesis and Action. *Plant Physiol.* **143**, 812–824.

Seemann, J.R. and Sharkey, T.D. (1987) The effect of abscisic acid and other inhibitors on photosynthetic capacity and the biochemistry of CO_2 assimilation. *Plant Physiol.* **84**, 696–700.

Shiferaw, B., Smale, M., Braun, H.-J., Duveiller, E., Reynolds, M. and Muricho, G. (2013) Crops that feed the world 10. Past successes and future challenges to the role played by wheat in global food security. *Food Sec.* **5**, 291–317.

Simkin, A.J., McAusland, L., Headland, L.R., Lawson, T. and Raines, C.A. (2015) Multigene manipulation of photosynthetic carbon assimilation increases CO_2 fixation and biomass yield in tobacco. *J. Exp. Bot.* **66**, 4075–4090.

Simmonds, J., Scott, P., Leverington-Waite, M., Turner, A.S., Brinton, J., Korzun, V., Snape, J. *et al*. (2014) Identification and independent validation of a stable yield and thousand grain weight QTL on chromosome 6A of hexaploid wheat (*Triticum aestivum* L.). *BMC Plant Biol.* **14**, 191.

Singh, D.K. and McNellis, T.W. (2011) Fibrillin protein function: the tip of the iceberg? *Trends Plant Sci.* **16**, 432–441.

Singh, D.K., Maximova, S.N., Jensen, P.J., Lehman, B.L., Ngugi, H.K. and McNellis, T.W. (2010) FIBRILLIN4 is required for plastoglobule development and stress resistance in apple and Arabidopsis. *Plant Physiol.* **154**, 1281–1293.

Sirhindi, G., Mushtaq, R., Gill, S.S., Sharma, P., Abd Allah, E.F. and Ahmad, P. (2020) Jasmonic acid and methyl jasmonate modulate growth, photosynthetic activity and expression of photosystem II subunit genes in *Brassica oleracea* L. *Sci. Rep.* **10**, 9322.

Sun, X., Cahill, J., Van Hautegem, T., Feys, K., Whipple, C., Novák, O., Delbare, S. *et al*. (2017) Altered expression of maize PLASTOCHRON1 enhances biomass and seed yield by extending cell division duration. *Nat. Commun.* **8**, 14752.

Sun, T., Yuan, H., Cao, H., Yazdani, M., Tadmor, Y. and Li, L. (2018) Carotenoid Metabolism in Plants: The Role of Plastids. *Mol. Plant* **11**, 58–74.

Sun, B., Jiang, M., Zheng, H., Jian, Y., Huang, W.-L., Yuan, Q., Zheng, A.-H. *et al*. (2020) Color-related chlorophyll and carotenoid concentrations of Chinese kale can be altered through CRISPR/Cas9 targeted editing of the carotenoid isomerase gene BoaCRTISO. *Hort. Res.* **7**, 161.

Tevini, M., & Steinmüller, D. (1985). Composition and function of plastoglobuli: II. Lipid composition of leaves and plastoglobuli during beech leaf senescence. *Planta*, **163**, 91–96.

Timm, S., Wittmiß, M., Gamlien, S., Ewald, R., Florian, A., Frank, M., Wirtz, M. *et al*. (2015) Mitochondrial dihydrolipoyl dehydrogenase activity shapes photosynthesis and photorespiration of *Arabidopsis thaliana*. *Plant Cell* **27**, 1968–1984.

Torres-Romero, D., Gómez-Zambrano, Á., Serrato, A.J., Sahrawy, M. and Mérida, Á. (2021) Arabidopsis fibrillin 1-2 subfamily members exert their functions via specific protein–protein interactions. *J. Exp. Bot.* **73**, 903–914.

Vidi, P.-A., Kessler, F., & Bréhélin, C. (2007). Plastoglobules: A new address for targeting recombinant proteins in the chloroplast. *BMC Biotechnol.* **7**, 4.

Wang, K., Li, M. and Hakonarson, H. (2010) ANNOVAR: functional annotation of genetic variants from high-throughput sequencing data. *Nucleic Acids Res.* **38**, e164.

Wasternack, C., Forner, S., Strnad, M. and Hause, B. (2013) Jasmonates in flower and seed development. *Biochimie* **95**, 79–85.

Xu, F., Fang, J., Ou, S., Gao, S., Zhang, F., Du, L., Xiao, Y. *et al*. (2015) Variations in *CYP78A13* coding region influence grain size and yield in rice. *Plant Cell Environ.* **38**, 800–811.

Yang, X., Pan, Y., Singh, P.K., He, X., Ren, Y., Zhao, L., Zhang, N. *et al*. (2019) Investigation and genome-wide association study for Fusarium crown rot resistance in Chinese common wheat. *BMC Plant Biol.* **19**, 153.

Youssef, A., Laizet, Y., Block, M.A., Maréchal, E., Alcaraz, J.-P., Larson, T.R., Pontier, D. *et al*. (2010) Plant lipid-associated fibrillin proteins condition jasmonate production under photosynthetic stress. *Plant J.* **61**, 436–445.

Ytterberg, A. J., Peltier, J.-B., & van Wijk, K. J. (2006). Protein profiling of plastoglobules in chloroplasts and chromoplasts. A surprising site for differential accumulation of metabolic enzymes. *Plant Physiol.* **140**, 984–997.

Zhai, H., Feng, Z., Du, X., Song, Y., Liu, X., Qi, Z., Song, L. *et al*. (2018) A novel allele of *TaGW2-A1* is located in a finely mapped QTL that increases grain weight but decreases grain number in wheat (*Triticum aestivum* L.). *Theor. Appl. Genet.* **131**, 539–553.

Zhang, X., Wang, J., Huang, J., Lan, H., Wang, C., Yin, C., Wu, Y. *et al*. (2012) Rare allele of *OsPPKL1* associated with grain length causes extra-large grain and a significant yield increase in rice. *PNAS* **109**, 21534–21539.

Zhu, X., Rong, W., Wang, K., Guo, W., Zhou, M., Wu, J., Ye, X. *et al*. (2021) Overexpression of *TaSTT3b-2B* improves resistance to sharp eyespot and increases grain weight in wheat. *Plant Biotech. J.* **20**, 777–793.

Zuo, J. and Li, J. (2014) Molecular genetic dissection of quantitative trait loci regulating rice grain size. *Annu. Rev. Genet.* **48**, 99–118.

Supporting information

Additional supporting information may be found online in the Supporting Information section at the end of the article.

Figure S1 Sequence alignment of *TaGL1-B1* in UC1110 and PI610750.
Figure S2 JA and ABA quantification in leaves of transgenic and mutant plants.
Figure S3 Relative expression level of *TaPAP6* in the mutants of *TaGL1* gene.
Figure S4 Relative expression level of JA- and ABA-related genes in leaves of *TaPAP6*-OE plants.
Figure S5 Relative expression level of TaPAP6 in seeds of *TaGL1-B1* overexpression lines.
Figure S6 The expression profile of *TaGL1-B1* and *TaPAP6* in diverse tissues at different developmental stages in common wheat.

Table S1 Two stable QTL on 1B for grain length in UP-RIL.
Table S2 Candidate genes in the 7.5-Mb interval on 1B.
Table S3 Gene markers for mapping *QKL.hau.1B*.
Table S4 Differential expression profile of 10 annotated genes identified in the target region of *QKL.hau.1B*.
Table S5 QTL re-mapping after adding *Ta90300* marker for grain length.
Table S6 Detailed information of Kronos mutants.
Table S7 Differentially expressed genes (DEGs) by RNA-seq in *TaPAP6*-OE and wild type.
Table S8 QTL mapping for carotenoid contents in the UP-RIL.
Table S9 DEGs involved in plant hormone metabolism between TaPAP6-OE and wild type.

